



EUROfusion

EUROFUSION WPSA-CP(16) 15080

M Romanelli et al.

Integrated modelling with JINTRAC of high- steady state scenarios in JT60SA

Preprint of Paper to be submitted for publication in
Proceedings of 26th IAEA Fusion Energy Conference



This work has been carried out within the framework of the EUROfusion Consortium and has received funding from the Euratom research and training programme 2014-2018 under grant agreement No 633053. The views and opinions expressed herein do not necessarily reflect those of the European Commission.

This document is intended for publication in the open literature. It is made available on the clear understanding that it may not be further circulated and extracts or references may not be published prior to publication of the original when applicable, or without the consent of the Publications Officer, EUROfusion Programme Management Unit, Culham Science Centre, Abingdon, Oxon, OX14 3DB, UK or e-mail Publications.Officer@euro-fusion.org

Enquiries about Copyright and reproduction should be addressed to the Publications Officer, EUROfusion Programme Management Unit, Culham Science Centre, Abingdon, Oxon, OX14 3DB, UK or e-mail Publications.Officer@euro-fusion.org

The contents of this preprint and all other EUROfusion Preprints, Reports and Conference Papers are available to view online free at <http://www.euro-fusionscipub.org>. This site has full search facilities and e-mail alert options. In the JET specific papers the diagrams contained within the PDFs on this site are hyperlinked

Investigation of Sustainable Reduced-Power non-inductive Scenarios on JT-60SA

M. Romanelli¹, P. Aresta-Belo¹, G. Corrigan¹, L. Garzotti¹, D. Harting¹, F. Koechl¹, S. Saarelma¹, S. Wiesen², M. Wischmeier³, R. Zagórski⁴, T. Bolzonella⁵, L. Pigatto⁵, J. Garcia⁶, P. Maget⁶, E. de la Luna⁷, N. Hayashi⁸, T. Nakano⁸, S. Ide⁸, M. Yoshida⁸, H. Urano⁸

¹ *Culham Centre for Fusion Energy, Culham Science Centre, Abingdon OX14 3DB, UK.*

² *Forschungszentrum Jülich GmbH, Institut für Energie- und Klimaforschung – Plasmaphysik, Partner of the Trilateral Euregio Cluster (TEC), 52425 Jülich, Germany*

³ *MPI für Plasmaphysik, Garching, Germany*

⁴ *Institute of Plasma Physics and Laser Microfusion, Hery 23, Warsaw, Poland*

⁵ *Consorzio RFX, I-35127 Padova, Italy*

⁶ *CEA, IRFM, F-13108 Saint-Paul-lez-Durance, France*

⁷ *Laboratorio Nacional de Fusión, CIEMAT, 28040, Madrid, Spain*

⁸ *National Institutes for Quantum and Radiological Science and Technology, Naka, Ibaraki, 311-0193, Japan*

e-mail contact of the main author: michele.romanelli@ccfe.ac.uk

Abstract. One of the main goals of JT-60SA will be the study of steady-state plasma scenarios characterised by high fractions of bootstrap current, low flux consumption and sustainable divertor heat-loads (Advanced Scenarios). The feasibility of the above scenarios will depend on the demonstration of simultaneous control of core / SOL / divertor conditions to achieve large core pressure / pressure-gradients and prevent impurity accumulation while ensuring an acceptable power load on the divertor targets. In this paper a high-beta scenario at 2.3MA, 1.7T with 17 MW of NBI heating and 7 MW of ECRH power has been investigated with the integrated suite of core / SOL / divertor codes JINTRAC. Various fuelling rates / locations have been simulated and it has been found that high values of beta and acceptable levels of power-load on the divertor outer-target can be achieved without impurity seeding for separatrix densities above $2 \times 10^{19} \text{ m}^{-3}$ and in condition of partial divertor detachment. The 0-D plasma parameters of the above reduced-power advanced scenario are discussed along with comparison against the reference values of the highest beta scenario in the JT-60SA research plan.

1. Introduction

Along with the construction and operation of ITER, the design of a demonstration thermonuclear fusion reactor (DEMO) is the main goal of current international fusion research. New generation of tokamaks as JT-60SA [1] are meant to provide important information to discriminate between different DEMO designs. In particular JT-60SA will explore steady-state plasma scenarios characterised by high fractions of non-inductive current and sustainable divertor heat-loads. The feasibility of the above scenarios will depend on the simultaneous control of core / SOL / divertor conditions to maintain a peaked pressure profile and a clean plasma while ensuring acceptable power loads on the divertor targets, not exceeding 10 MWm^{-2} . The high- β steady-state scenarios of JT-60SA are designed to be achievable through high plasma shaping and might rely on the triggering of an internal transport barrier that together with the external barrier will ensure high confinement. Detailed core transport studies of the above scenarios have been carried out with multiple codes and transport models indicating that steady state conditions with the 0-D parameters reported in the research plan should be achievable when pedestal pressure values within the stability limits are reached [2,3,4]. However preliminary investigations with SONIC and COREDIV of

the SOL / divertor conditions show that without impurity seeding the sustainment of the highest beta reference scenario at 2.3MA, 1.7T will be challenging due to the large divertor power-loads which are predicted when 30 MW NBI power plus 7 MW of ECRH power are employed [5,6]. Further studies have confirmed that impurity seeding (e.g. Ar) is likely to reduce the divertor power-load to sustainable levels and enable operation at the nominal heating power. On the other hand before attempting to mitigate the divertor power load via seeding in the full power scenario it will be necessary to develop and operate a reduced-power optimised scenario where both the fraction of non-inductive current and beta are maximised while the heat flux to the divertor is kept at a sustainable level. A reduced-power scenario has been investigated with the integrated suite of codes JINTRAC [7] where a core transport code JETTO is coupled to a SOL / divertor code EDGE2D in tokamak realistic geometry. Neutral density is computed by the Monte Carlo code EIRENE for both deuterium and impurities. The NBI power deposition is computed self consistently by the PENCIL code. The ECRH power density profile is assumed as a Gaussian localised at the resonant surface and it is not calculated self-consistently in the simulation. The pedestal height is modelled via the continuous ELM model and α_c is compared with ELITE / MISHKA calculation. The consistency between imposed pedestal width and predicted height has also been checked with the EPED model. The sensitivity of the pedestal prediction to plasma parameters has been investigated via parameter scans around the design point. The above simulations allow accounting for the full SOL / divertor geometry and consistent coupling of fluxes and separatrix conditions between core and edge. The flexibility in defining the position of gas injection valves allows assessing the impact on the divertor heat load of fuelling from different locations.

2. JINTRAC Modelling Assumptions

Core / edge coupled simulations have been performed for the 2.3MA, 1.7T steady-state high beta non-inductive scenario starting from the steady-state JETTO core simulation presented in [2,3] for the 37 MW (30 MW NBI + 7 MW ECRH) scenario 5.1 of the JT-60SA research plan [1], and an additional core simulation performed with 24 MW of auxiliary heating (17 MW NBI + 7 MW of ECRH). The core transport model chosen is Bohm/gyro-Bohm and an internal transport barrier develops at $r/a = 0.5$ where the transport coefficients are reduced to the level of 10% the BgB local conductivity. The external transport barrier extends inside the plasma for 4 cm from the separatrix and neoclassical heat and particle transport is assumed within the barrier region with an additional anomalous transport to keep the pressure gradient at the critical value. The transport in the SOL is set up to match the settings of SONIC simulations for the same scenario [4], namely electron and ion perpendicular conductivity of $1.0 \text{ m}^2\text{s}^{-1}$ and perpendicular particle diffusivity of $0.3 \text{ m}^2\text{s}^{-1}$. The pumping rate of the divertor cryopump is taken to be $50 \text{ m}^3/\text{s}$. Figure 1 and 2 show the grids adopted in the simulations for EDGE2D and EIRENE respectively. Fuelling of the plasma is achieved via recycling at the wall / divertor-plates and via deuterium puff from different locations and different puffing rates, leading to different separatrix densities. Carbon is included in the simulations as main impurity and both chemical and physical sputtering at different rates is taken into account. The coupling between core and edge occurs at the first inner ring of EDGE2D where the fluxes calculated by JETTO are used as boundary conditions for the edge code, while flux averaged densities and temperatures calculated by EDGE2D are used as boundary conditions for JETTO / SANCO. It is important to point out that while in ordinary SOL / divertor simulations the fluxes at the boundary are set externally, in the core / SOL coupled simulations they are the result of the core transport.

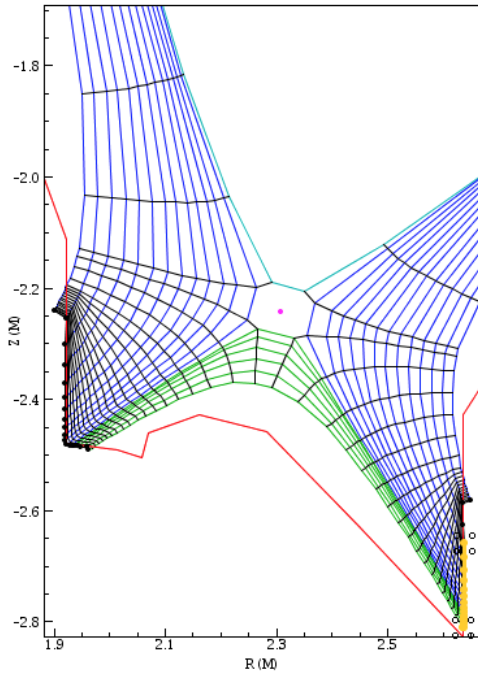


Fig. 1: EDGE2D grid used in the coupled edge / core simulations and puffing region at divertor target (yellow line)

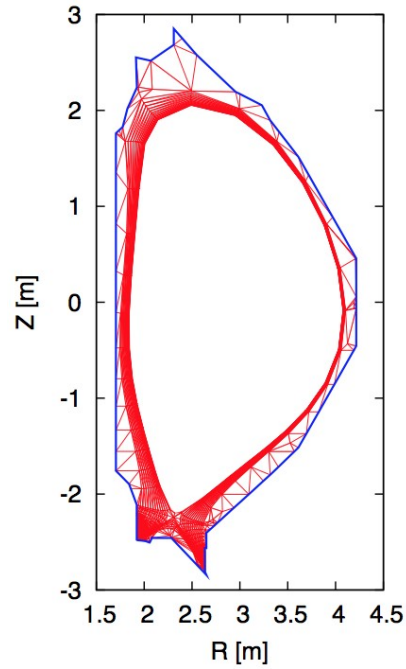


Fig. 2 EIRENE grid used in the coupled edge / core simulations.

Fully coupled simulations using a variable time step (in average of the order of 10^{-6} s) have been executed for the equivalent of 700ms of plasma time to allow the SOL to relax and the core to fully equilibrate with the new boundary conditions.

3. JINTRAC Simulations of JT-60SA high beta scenarios

Fully coupled core / SOL / divertor simulations of the reference high power non-inductive scenario (30 MW NBI + 7 MW ECRH) have been performed with different puffing and recycling rates leading to different values of the electron-density at the separatrix, and different carbon sputtering rates to account for non simulated mechanisms such as ELMs. Four simulations are reported here illustrating the scaling of the power-load to targets with electron density. The first simulation (blue profile in Fig. 3, 4) has been obtained with a mid-plane puff, maximum control rate $5.0 \times 10^{21} \text{ s}^{-1}$, electron-density at separatrix $2.0 \times 10^{19} \text{ m}^{-3}$, $50 \text{ m}^3 \text{ s}^{-1}$ divertor pumping; this simulation shows the highest power load on the inner / outer-target and lowest separatrix density; the second simulation (black profile in Fig. 3, 4) is obtained by puffing gas from the mid-plane, maximum control rate $1.0 \times 10^{22} \text{ s}^{-1}$, electron-density at the separatrix $3.0 \times 10^{19} \text{ m}^{-3}$, $50 \text{ m}^3 \text{ s}^{-1}$ divertor pumping; the third simulation (red profile in Fig. 3, 4) is obtained with mid-plane puff, maximum control rate $5.0 \times 10^{21} \text{ s}^{-1}$, electron density at the separatrix $3.5 \times 10^{19} \text{ m}^{-3}$; finally the fourth simulation (green profile in Fig. 3, 4) is from a mid-plane puff, maximum control rate $5.0 \times 10^{21} \text{ s}^{-1}$, electron density at the separatrix $3.5 \times 10^{19} \text{ m}^{-3}$; this simulation has the minimum power load on the outer-target. All simulations find a strong difference between power deposited on the divertor inner- (more than one order of magnitude lower) and outer- target.

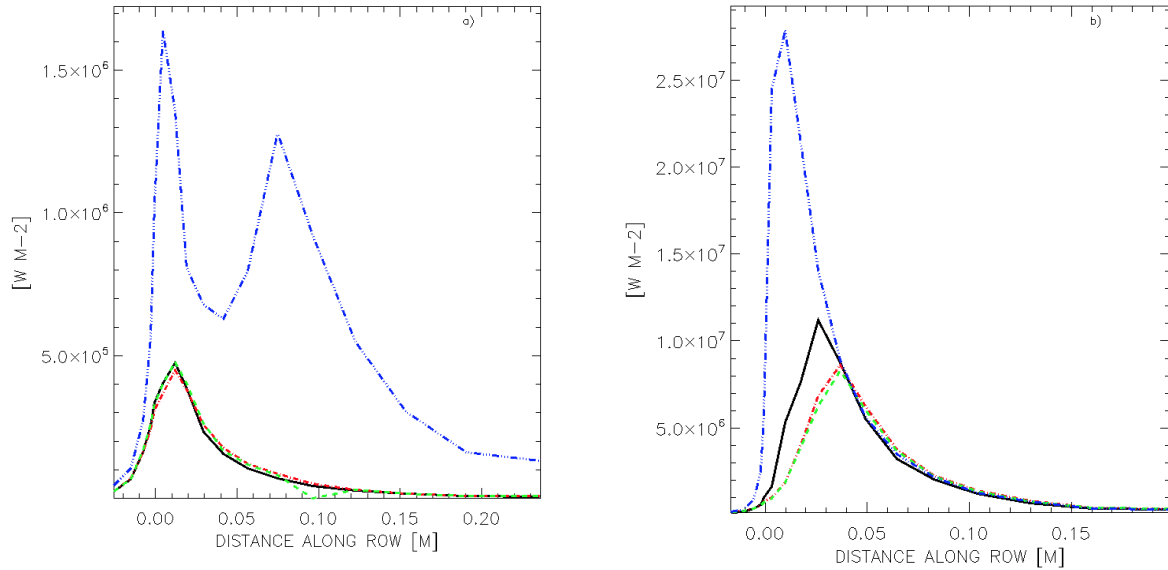


Fig. 3: Total power deposited on the inner divertor-target a) and outer divertor-target b) vs. distance from the strike point for different levels of gas puff and puffing positions: blue profile has been obtained with a mid-plane puff, maximum control rate $5.0 \times 10^{21} \text{ s}^{-1}$, electron-density at separatrix $2.0 \times 10^{19} \text{ m}^{-3}$, $50 \text{ m}^3 \text{ s}^{-1}$ divertor pumping; black profile is obtained by puffing gas from the mid-plane, maximum control rate $1.0 \times 10^{22} \text{ s}^{-1}$, electron-density at the separatrix $3.0 \times 10^{19} \text{ m}^{-3}$, $50 \text{ m}^3 \text{ s}^{-1}$ divertor pumping; red profile is obtained with mid-plane puff, maximum control rate $5.0 \times 10^{21} \text{ s}^{-1}$, electron density at the separatrix $3.5 \times 10^{19} \text{ m}^{-3}$; green profile is from a mid-plane puff, maximum control rate $5.0 \times 10^{21} \text{ s}^{-1}$, electron density at the separatrix $3.5 \times 10^{19} \text{ m}^{-3}$;

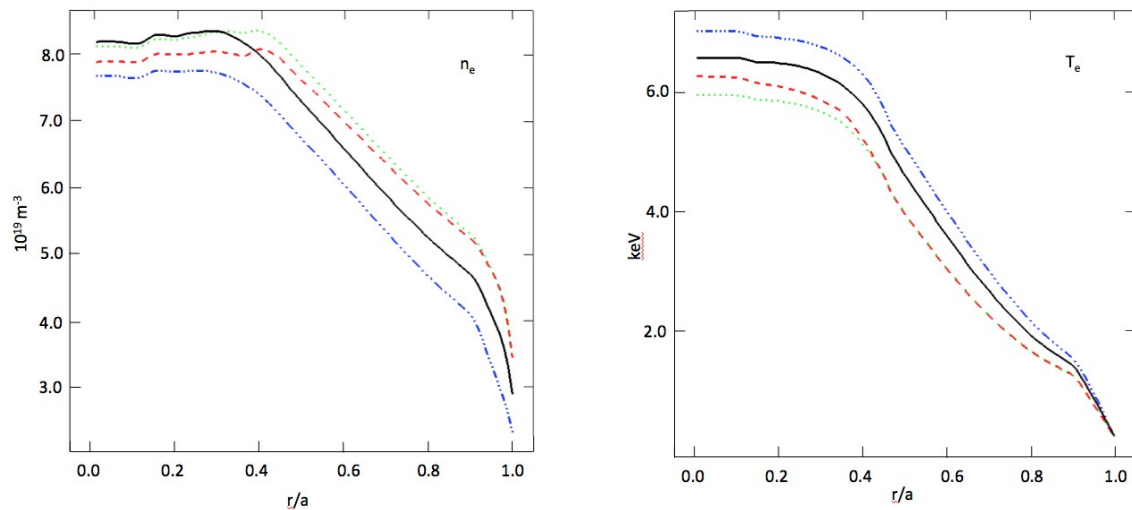


Fig. 4: Electron density profiles (left) and electron temperature profiles (right) vs. JETTO normalised plasma minor radius at steady state for the different levels of gas puff / puffing positions: same colour code as in Fig. 3.

The simulations above show an increasing degree of detachment at the inner target with increasing electron density. All simulations reach a beta normalised above 4, full non-inductive current drive with Z_{eff} of 1.6 and Greenwald fractions of order 1.0. The above simulations confirm previous results of SONIC and COREDIV namely that impurity seeding will be needed to mitigate the divertor power-load in this high-power scenario when operating at low densities. Operation without impurity seeding might be possible at high densities, close to the Greenwald limit (electron density at the separatrix above $2 \times 10^{19} \text{ m}^{-3}$), in conditions of plasma detached from the divertor inner-target.

Fully coupled core / SOL / divertor simulations of a reduced-power version of the high beta scenario 2.3MA/1.7T, with 5 MW negative-ion NBI power off-axis and 12 PNBI + 7 MW ECRH, have been performed with different puffing levels/locations and recycling rates leading to different values of the electron-density at the separatrix, and different carbon sputtering rates to allow for non simulated mechanisms such as ELMs. Four simulations are reported here. The results are summarised in Figures 7 and 8 as follows: the first simulation (red profile in Fig. 5, 6, Simulation 1 in Table 1) is obtained by puffing gas from the X-point private region near the target, maximum control rate $3.6 \times 10^{22} \text{ s}^{-1}$, electron density at the separatrix $2.2 \times 10^{19} \text{ m}^{-3}$, $50 \text{ m}^3 \text{ s}^{-1}$ divertor pumping; the second simulation (green profile in Fig. 5, 6, Simulation 2 in Table 1) is obtained with mid-plane puff, maximum control rate $3.6 \times 10^{22} \text{ s}^{-1}$, electron density at the separatrix $2.2 \times 10^{19} \text{ m}^{-3}$; the third simulation (blue profile in Fig. 5, 6, Simulation 3 in Table 1) has been obtained with an increased mid-plane gas puff, maximum control rate $3.0 \times 10^{21} \text{ s}^{-1}$, electron density at the separatrix $2.8 \times 10^{19} \text{ m}^{-3}$, $50 \text{ m}^3 \text{ s}^{-1}$ divertor pumping; finally the fourth simulation (black profile in Fig. 5, 6, Simulation 4 in Table 1) is obtained by puffing gas from the mid-plane, maximum control rate $3.6 \times 10^{22} \text{ s}^{-1}$, electron-density at the separatrix $2.0 \times 10^{19} \text{ m}^{-3}$, $50 \text{ m}^3 \text{ s}^{-1}$ divertor pumping and decreased carbon sputtering rate. The simulations with highest SOL / separatrix densities show partial/full detachment as indicated by the ion temperature profiles at the inner target, Fig. 7. The level of non-inductive current is illustrated in Fig. 8 and Fig. 9 shows the q profile (similar in all simulations).

All simulations find a strong difference between power deposited on the divertor inner- (one order of magnitude lower) and outer- target. The 0-D core plasma parameters of the four simulations are reported in Table 1.

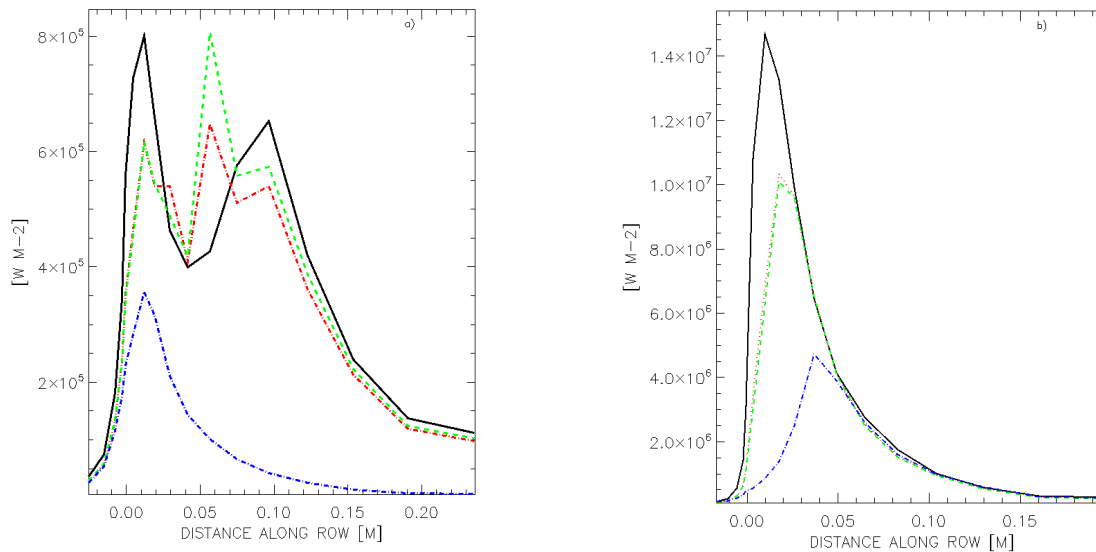


Fig. 5: Total power deposited on the inner divertor-target a) and outer divertor-target b) vs. distance from the strike point for different levels of gas puff and puffing positions: red profile, puff from the X-point private region near the target, maximum control rate $3.6 \times 10^{22} \text{ s}^{-1}$, electron-density at the separatrix $2.2 \times 10^{19} \text{ m}^{-3}$, $50 \text{ m}^3 \text{ s}^{-1}$ divertor pumping; green profile, mid-plane puff, maximum control rate $3.6 \times 10^{22} \text{ s}^{-1}$, electron-density at the separatrix $2.2 \times 10^{19} \text{ m}^{-3}$; blue profile, increased mid-plane gas puff, maximum control rate $3.0 \times 10^{21} \text{ s}^{-1}$, electron-density at the separatrix $2.8 \times 10^{19} \text{ m}^{-3}$, $50 \text{ m}^3 \text{ s}^{-1}$ divertor pumping; black profile, puff from the mid-plane, maximum control rate $3.6 \times 10^{22} \text{ s}^{-1}$, electron-density at the separatrix $2.0 \times 10^{19} \text{ m}^{-3}$, $50 \text{ m}^3 \text{ s}^{-1}$ divertor pumping and lower carbon concentration in the SOL.

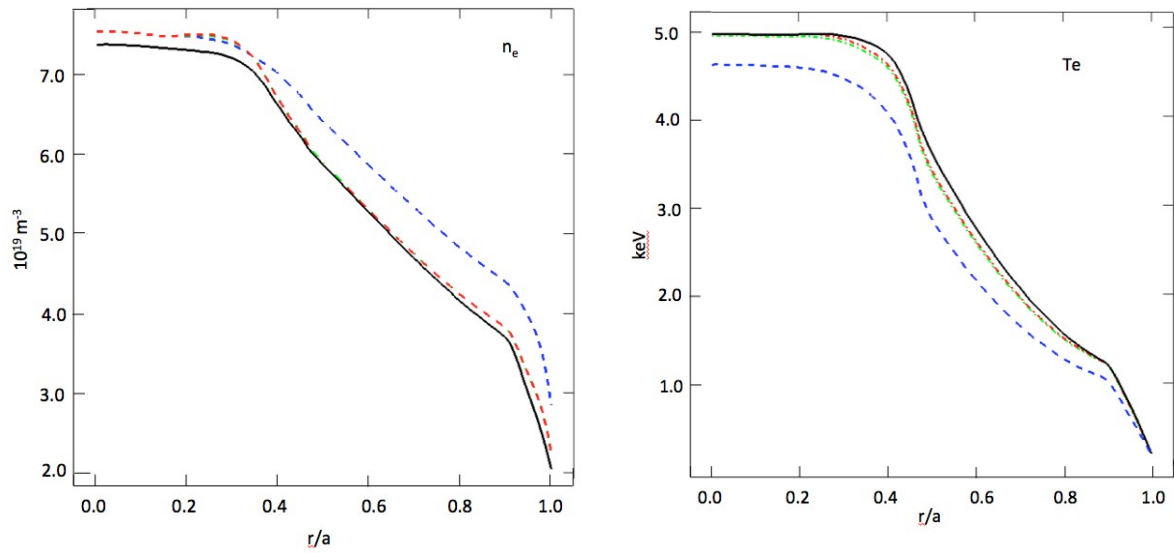


Fig. 6: Electron density profiles (left) and electron temperature profiles (right) vs. JETTO normalised plasma minor radius at steady state for the different levels of gas puff and puffing positions: same colour code as in Fig. 5.

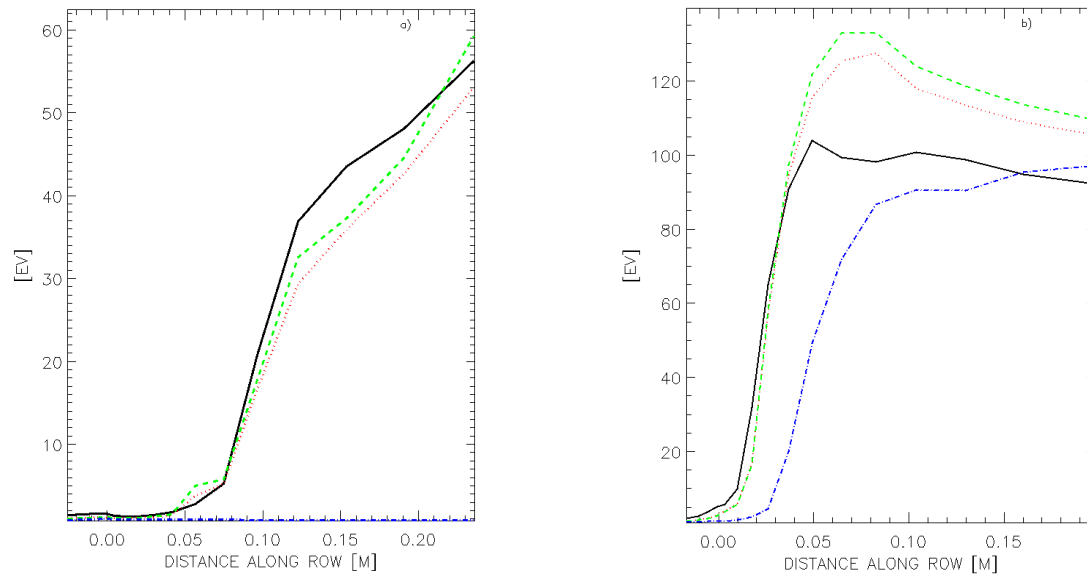


Fig. 7: Ion temperature profiles on the inner divertor-target a) and outer divertor-target b) vs. distance from the strike point for different levels of gas puff and puffing positions: same colour code as in Fig 5.

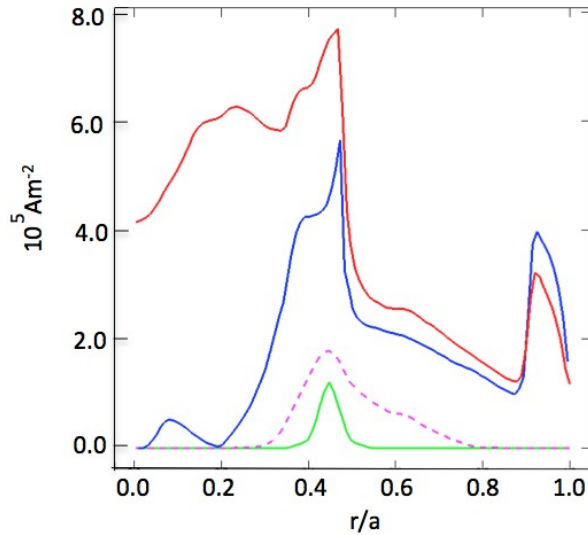


Fig. 8 red profile total current density, blue bootstrap current, dashed-purple NBI driven current, green ECH driven current.

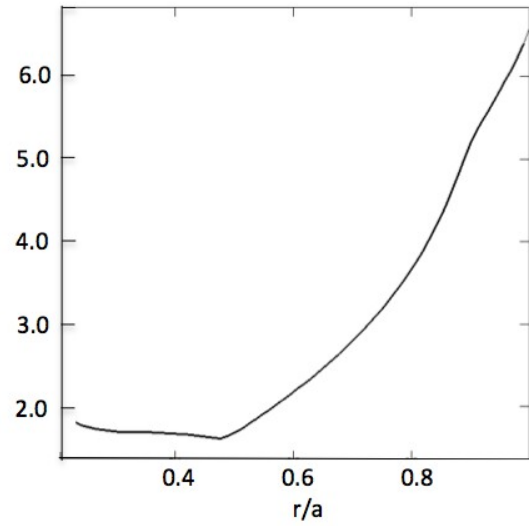


Fig. 9 typical q profile found in the reduced power simulations (central value near 4, not shown here).

	Non-inductive current	β_N	Z_{eff}	f_{GW}	$n_{e,\text{sep}}/n_{D,\text{sep}}$ (10^{19} m^{-3})	Peak Power load on outer-target [MW m^2]
Scenario 5.1	100%	4.3	2.0	0.85	1.7/1.0	n.a.
Simulation 1	74%	3.7	1.7	0.97	2.2/2.0	10
Simulation 2	74%	3.6	1.7	0.94	2.2/2.0	10
Simulation 3	64%	3.6	1.6	0.99	2.8/2.4	4
Simulation 4	74%	3.7	1.4	0.95	2.0/1.7	14

Table 1. Summary of the 0-D plasma parameters from the simulations of the reduced-power (24 MW) non-inductive scenario: Simulation 1, red profile of Fig. 5; Simulation 2, green profile of Fig. 5; Simulation 3, blue profile of Fig. 5; Simulation 4, black profile of Fig. 5.

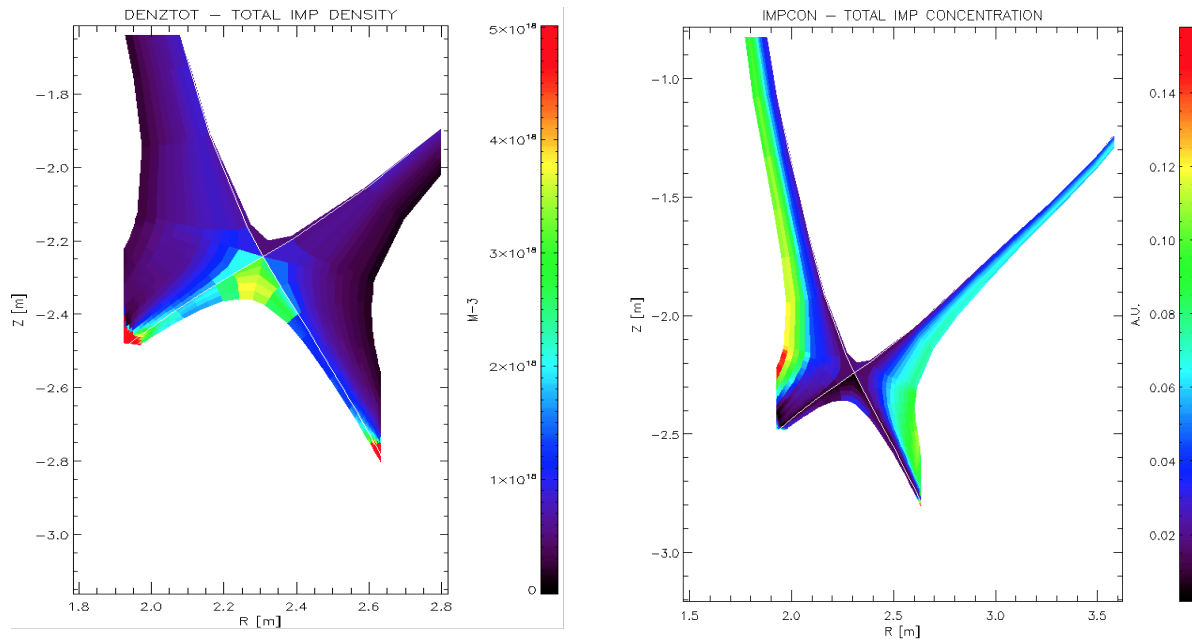


Fig. 10 Simulation 2, total carbon density (all ionisation states) in the divertor region (left) and carbon concentration in the SOL.

Figure 10 shows the carbon density (all ionisation states) in the divertor region and the concentration in the SOL for Simulation 2 of Table 1. A larger concentration of carbon is found at the high field side and a large carbon density in the private region below the X-point.

4. Summary and Conclusions

Fully coupled Core / SOL / divertor simulations of the JT-60SA high- β non-inductive scenario have been performed for the first time with the JINTRAC code. Investigation of the full power reference scenario 2.3MA/ 1.7T with 37 MW of auxiliary heating find similar results as SONIC and CORDIV, namely a power-load on the divertor outer-target in excess of 25 MWm⁻² is found for an electron-separatrix density of 2.0×10^{19} m⁻³. The power load to both targets is found to decrease with increased separatrix density. Plasma detachment at the divertor inner-target starts to appear for separatrix densities above 3.0×10^{19} m⁻³. Operation of the full power scenario with detached plasma at the inner-target would provide 100% non inductive current and beta above 4 however it will require working at high densities close or above the Greenwald limit.

When the auxiliary power employed in the 2.3MA/ 1.7T scenario is reduced to 24 MW it is found that the power-load to the outer-target can be more easily reduced to (or maintained below) 10 MWm⁻² by adopting both mid-plane and target gas-puff. The reduction of the power-load on the divertor targets is due to the combination of increased electron separatrix-density that leads to higher carbon spattering and radiation. As a consequence of operating at high density the fraction of non-inductive current is reduced to 74% and the Greenwald fraction is increased above 90%. The best performance at lower power is achieved with a maximum fuel-control-rate of 3.6×10^{22} s⁻¹, puffing from the mid-plane, leading to a partially detached divertor, plasma beta normalized of 3.7 and a fraction of non-inductive current of 74%.

Acknowledgement: This work has been carried out within the framework of the EUROfusion Consortium and has received funding from the Euratom research and training programme 2014-2018 under grant agreement No 633053. The views and opinions expressed herein do not necessarily reflect those of the European Commission. The authors gratefully acknowledge members of the JT-60SA Integrated Project Team for data exchange and fruitful discussions.

- [1] JT-60SA Research Plan, http://www.jt60sa.org/pdfs/JT-60SA_Res_Plan.pdf, March (2016)
- [2] L Garzotti, 8th IAEA Technical Meeting, Nara, Japan (2015)
- [3] S. Ide *et al*, Proceedings of the 2016 EPS conference
- [4] G. Giruzzi *et al*, IAEA FEC 2016, EX-P8/40
- [5] R. Zagórski *et al*, 2016 *Nucl. Fusion* **56** 016018
- [6] K. Hoshino *et al*, *Contrib. Plasma Phys.* 54 (2014) 404
- [7] M Romanelli *et al*, *Plasma and Fusion Res.* Volume 9, 3403023 (2014)